GANIT *J. Bangladesh Math. Soc.* (ISSN 1606-3694) **36** (2016) 7-17

EFFECT OF RADIATION AND HEAT GENERATION ON UNSTEADY MHD FLOW OF NON-NEWTONIAN FLUID ALONG A STRETCHING VERTICAL SURFACE

Shirin Provat[1], M. R. Hossain[2,*] and M. A. Samad[3]
[1]Department of Basic Sciences and Humanities, University of Asia Pacific, Dhaka, Bangladesh
[2, 3]Department of Applied Mathematics, University of Dhaka, Bangladesh
[*]Corresponding author: mrhossain@du.ac.bd

Received 05.07.2015 Accepted 28.08.2016

ABSTRACT

In this paper, the unsteady forced convection boundary-layer flow of a non-Newtonian fluid along a continuously moving stretching sheet with thermal radiation and heat generation or absorption in the presence of magnetic field has been studied. First, the governing equations have been non-dimensionalized by usual transformations to obtain the similar solutions. Then, the obtained equations have been solved by an implicit finite difference method. The convergency of explicit and implicit finite difference method has also been discussed. The results are presented for the effect of various parameters such as magnetic parameter (M), radiation parameter (N), heat source parameter (Q), Prandtl number (Pr) and power-law fluid index (n). The effects of these parameters on skin-friction coefficient (C_f) and the local Nusselt number (N_{u_L}) which are of physical and engineering interest have also been studied and presented graphically.

Keywords: Unsteady MHD flow, Non-Newtonian fluid, Heat generation/absorption, Radiation

1. Introduction

Over recent years, applications of non-Newtonian fluids in many industrial processes have been an interesting topic to many researchers. Different models have been proposed to explain the behavior of non-Newtonian fluid. Schowalter [1] was the first one, who formulated the boundary layer flow of a Non-Newtonian fluid. The study of flow and heat transfer generated by stretching surface plays a significant role in many material processing applications such as hot rolling, extrusion, metal forming, wire and glass fiber drawing and continuous casting. Numerous investigations like Banks [2] and Chen [3] were done on the stretching sheet problem with linear stretching in different directions in the absence of the magnetic field.

The study of effects of magnetic field on free convection flow is important in liquid-metals, electrolytes and ionized gases. Kishan and Sashidhar [4] analyzed the momentum and heat transfer in laminar boundary layer flow of non- Newtonian fluids past a semi-infinite flat plate with the thermal dispersion in the presence of a uniform magnetic field for both the cases of static plate and continuous moving plate. However, at present, the radiation effect on MHD flow and heat transfer problems has become more important industrially.

Effects of radiation on non-Newtonian fluids have been studied by many authors like Sahoo and Poncet [5] and Sajidand Hayat [6]. All the above mention studies consider the steady-state problem. But in certain practical problems, the motion of the stretched surface may start from the rest. In these problems, the transient or unsteady aspects become more interesting. The unsteady heat transfer problems over a stretching surface, which is started impulsively from restore is stretched with a velocity that depends on time, are considered. Elbashbeshy and Bazid [7] presented an exact similarity solution for unsteady momentum and heat transfer flow whose motion is caused solely by the linear stretching of a horizontal stretching surface. In the case of unsteady boundary-layer flow, Singh [8] investigated the thermal radiation and magnetic field effects on an unsteady stretching permeable sheet in the presence of free stream velocity. Later, Gamal and Abdel-Rahman [9] analyzed the effects of variable viscosity and thermal conductivity on unsteady MHD non-Newtonian flow over a stretching porous sheet.

In this present study, we have studied the effects of forced convection on unsteady magneto-hydrodynamic (MHD) non-Newtonian fluid flow along a vertical, continuously moving stretching sheet with radiation and heat generation or absorption. Firstly, the governing nonlinear partial differential equations are transformed into a system of dimensionless nonlinear partial differential equations using appropriate transformations. Then the resulting non-linear equations are solved numerically using both an explicit and an implicit finite difference technique. A comparison is also presented between these two schemes based on the convergence. Later, a parametric study has been carried out to explore the effect of some physically important parameters such as magnetic parameter (M), radiation parameter (N), heat source parameter (Q), Prandtl number (Pr) and power-law fluid index (n) on momentum and thermal boundary layers. The effects of these parameters on skin-friction coefficient (C_f) and the local Nusselt number (N_{u_L}) have also been discussed.

2. Mathematical Analysis

Consider the unsteady MHD forced convection laminar boundary layer flow of a viscous, incompressible non-Newtonian fluid past a continuously moving stretched surface in the vertical direction under the influence of thermal radiation and heat generation or absorption.

The frame of reference is chosen such that stretching surface coincides with the plane Y where the flow is assumed only for Y > 0. Introducing the Cartesian co-ordinate system, the X-axis is taken along the stretching surface in the vertically upward direction and the Y-axis is taken as normal to the surface. Two equal and opposite forces are introduced along the X-axis so that the surface is stretched, keeping the origin fixed.

An external magnetic field is applied in the Y-direction. Since we have taken the fluid to be the electrically conducting, hence we can neglect the effect of the induced magnetic field in comparison to the applied magnetic field. Therefore, only the applied magnetic field B_0 plays a

role which gives rise to magnetic force $F_x = \frac{\sigma B_0{}^2 u}{\rho}$ in the X-direction.

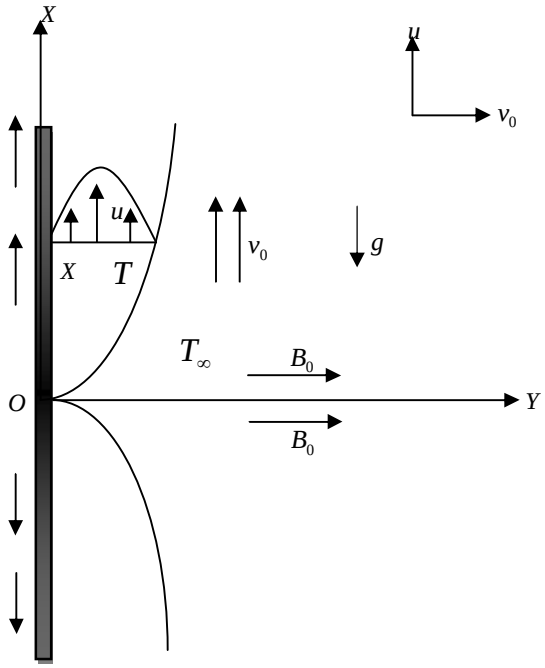

Fig. 1: Physical model and co-ordinate system

Since, we are considering forced convection, there is no influence of temperature field on velocity field i.e. there is no bouncy force. The Rosseland approximation (Rohsenow [10]) is used to describe the radioactive heat flux q_r in the energy equation. The radioactive heat flux in the X-direction is considered negligible in comparison to the Y-direction. The physical configuration and coordinate system is shown in Figure 1.

Under the above assumptions and the usual boundary layer approximation, the unsteady MHD forced convection non-Newtonian fluid flow with heat and the radiation effect are governed by the following equations:

Continuity equation:

$$\frac{\partial v_0}{\partial y} = 0 \tag{1}$$

Momentum equation:

$$\rho\left(\frac{\partial u}{\partial t} + v_0 \frac{\partial u}{\partial y}\right) = K \frac{\partial}{\partial y}\left(\left|\frac{\partial u}{\partial y}\right|^{n-1} \frac{\partial u}{\partial y}\right) - \sigma B_0{}^2 u \tag{2}$$

Energy equation:
$$\rho C_p\left(\frac{\partial T}{\partial t}+v_0\frac{\partial T}{\partial y}\right)=\kappa\frac{\partial^2 T}{\partial y^2}+Q_0\left(T-T_\infty\right)-\frac{\partial q_r}{\partial y} \tag{3}$$

The initial and boundary conditions are:

Initial conditions:
$$u=0,\quad T=0 \qquad \text{at } t=0 \tag{4}$$

Boundary conditions:
$$\left.\begin{array}{ll} u=U_0, & T=T_w \quad \text{when } y=0 \\ \text{and } u=0, & T=T_\infty \quad \text{when } y\to\infty \end{array}\right\} \quad \text{at } t>0 \tag{5}$$

Where, u and v_0 are the velocity components in the X and Y direction respectively, t is for time, T represents temperature field, U_0 and T_∞ are velocity and temperature of free stream, T_w is temperature at the surface, ρ is the fluid density, K is the consistency coefficient, σ is the electric conductivity, B_0 is the magnetic field, n is the power-law fluid index, C_p is the specific heat at constant pressure, κ is the thermal conductivity of the fluid, Q_0 is the volumetric rate of heat generation or absorption and q_r is the radioactive heat flux.

By using the Rosseland approximation, the radioactive heat flux q_r is,
$$q_r=-\frac{4\sigma_s}{3k_e}\frac{\partial T^4}{\partial y} \tag{6}$$

Where, σ_s is the Stefan–Boltzmann constant and k_e is the mean absorption coefficient.
If the temperature differences within the flow are sufficiently small, then Eq.(6) can be linearized by expanding T^4 in a Taylor series about T_∞, which after neglecting higher order terms takes the form,
$$T^4\approx 4T_\infty{}^3T-3T_\infty{}^4 \tag{7}$$

Therefore, using (6) and (7), we have
$$\frac{\partial q_r}{\partial y}=-\frac{16\sigma_s T_\infty{}^3}{3k_e}\frac{\partial^2 T}{\partial y^2} \tag{8}$$

Finally, using (8) in the energy equation (3), the governing boundary layer equations become,

Continuity equation:
$$\frac{\partial v_0}{\partial y}=0 \tag{9}$$

Momentum equation:
$$\frac{\partial u}{\partial t}+v_0\frac{\partial u}{\partial y}=\frac{K}{\rho}\frac{\partial}{\partial y}\left(\left|\frac{\partial u}{\partial y}\right|^{n-1}\frac{\partial u}{\partial y}\right)-\sigma\frac{B_0{}^2u}{\rho} \tag{10}$$

Energy equation:
$$\frac{\partial T}{\partial t}+v_0\frac{\partial T}{\partial y}=\alpha\frac{\partial^2 T}{\partial y^2}+\frac{Q_0}{\rho C_p}\left(T-T_\infty\right)+\frac{16\sigma_s T_\infty{}^3}{3k_e\rho C_p}\frac{\partial^2 T}{\partial y^2} \tag{11}$$

Subject to the initial condition (4) and boundary condition (5). Where, α is the thermal diffusivity. To make the governing equations dimensionless introducing the following dimensionless variables,
$$Y=\frac{y}{L},\ U=\frac{u}{U_0},\ V=\frac{v_0}{U_0},\ \bar{t}=\frac{tU_0}{L},\ \overline{\mathrm{T}}=\frac{T-T_\infty}{T_w-T_\infty} \tag{12}$$

Where, L is the characteristic length.

The nonlinear coupled partial differential equations in terms of dimensionless variables are,

Continuity equation:
$$\frac{\partial V}{\partial Y} = 0 \tag{13}$$

Momentum equation:
$$\frac{\partial U}{\partial t'} + V\frac{\partial U}{\partial Y} = \frac{1}{\mathrm{Re}}\frac{\partial}{\partial Y}\left(\left|\frac{\partial U}{\partial Y}\right|^{n-1}\frac{\partial U}{\partial Y}\right) - MU \tag{14}$$

Energy equation:
$$\frac{\partial \bar{T}}{\partial \bar{t}} + V\frac{\partial \bar{T}}{\partial Y} = \frac{1}{\mathrm{Re}\,\mathrm{Pr}}\left(1+\frac{4}{3\mathrm{N}}\right)\frac{\partial^2 \bar{T}}{\partial Y^2} + Q\bar{T} \tag{15}$$

With initial and boundary equations:

Initial conditions:
$$U = 0,\ \bar{T} = 0 \ \text{ at } \bar{t} = 0 \tag{16}$$

Boundary conditions:
$$\left.\begin{array}{lll} U = 1,\ \bar{T} = 1 & \text{when} & Y = 0 \\ \text{and} \quad U = 0,\ \bar{T} = 0 & \text{when} & Y \to \infty \end{array}\right\} \quad \text{at } \bar{t} > 0 \tag{17}$$

Where, the local Reynolds number, $\mathrm{Re} = \dfrac{U_0^{\,2-n}L^n}{K/\rho}$, the heat source parameter, $Q = \dfrac{Q_0 L}{\rho C_p U_0}$,

the generalized Prandtl number, $\mathrm{Pr} = \dfrac{K/\rho}{\alpha}\left(\dfrac{U_0}{L}\right)^{n-1}$, the radiation number, $\mathrm{N} = \dfrac{k_e\kappa}{4\sigma_s T_\infty^{\,3}}$

and the magnetic field parameter, $M = \dfrac{\sigma B_0^{\,2}}{\rho}\dfrac{L}{U_0}$

Dimensionless skin friction coefficient (C_f) and the local Nusselt number (Nu_L) are,

$$C_f = \frac{\tau_w}{\frac{1}{2}\rho U_0^{\,2}} \quad \text{or, } C_f = \frac{2}{\mathrm{Re}}\left|\frac{\partial U}{\partial Y}\right|^n\Bigg|_{Y=0} \tag{18}$$

$$Nu_L = \frac{hL}{\kappa} \qquad \text{or, } \quad Nu_L = -\frac{\partial \bar{T}}{\partial Y}\Bigg|_{Y=0} \tag{19}$$

3. Numerical Computation

For solving the governing equations (13)-(15) subject to the initial conditions (16) and boundary conditions (17) finite difference method is used. Both explicit and implicit difference scheme are used to approximate the solution of momentum equation (14) and only explicit difference scheme is used to approximate the solution of energy equation (15).

For this, a rectangular region of the flow field is chosen, where the X-axis is taken along the stretching surface and the Y-axis is normal to the plate. Grids along Y-axis represent time steps. Here, we consider that the length of the sheet is X_{max} (= 20), i.e. x varies from 0 to X_{max}. There are N_x (= 200) and N_t (= 1000000) grid spacing in the X and Y directions, respectively. And the mesh size along X and Y-axis are Δx and $\Delta t = k = 0.000001$ respectively. From continuity equation (13) we can consider V as a constant velocity.

For solving momentum equation in explicit difference technique, we will use a 2-point forward

difference approximation for time derivative and central difference approximation for spatial derivatives. While in implicit finite difference method, 2-point backward difference approximation is used to approximate time derivative and central difference approximations are used to approximate spatial derivatives. Here, $\left|\frac{\partial U}{\partial Y}\right|^{n-1}$ is approximated by the 2-point central difference approximation at the previous time step to avoid nonlinearity. The obtained system of linear equations is solved using Gauss-Seidel iterative technique.

For approximating the solution of the energy equation, 2-point forward difference approximation is used for time derivative and central difference approximation for spatial derivatives.

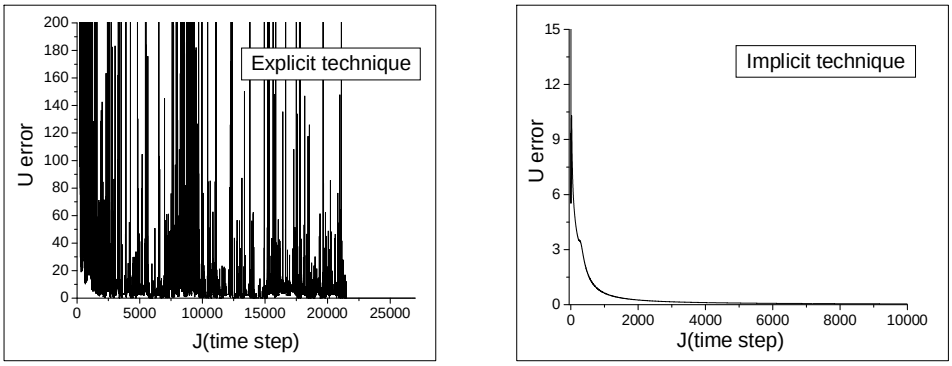

Fig. 2: Velocity error covergency profile in explicit and implicit method.

The same values of all the parameters and constants have been used in both techniques. Here we have acquired a convergency of 10^{-4} . In implicit technique, the error converges exponentially to zero almost after time steps j = 1000 while in explicit method after numerous fluctuation the error converges to zero after time steps j = 22000 (Fig. 2). Therefore, velocity error converges to zero faster in implicit method than in explicit method. Now we will do our further analysis by using implicit technique.

4. Results and Discussion

The system of non-linear partial differential equations (13)-(15) are solved under initial and boundary conditions (16) and (17) by using implicit finite difference scheme along with Gauss-Seidel iteration method. Numerical results are obtained for various values of magnetic parameter (M), radiation parameter (N), Prandtl number (Pr), heat source parameter (Q) and power-law fluid index (n) to study the effects of these parameters on momentum and thermal boundary layers as well as on skin friction coefficient (C_f) and the local Nusselt number (N_{u_L}). The graphs are plotted for dimensionless velocity (U) and temperature (T) at dimensionless time $\bar{t} = 1$.

Fig.3 represents the velocity distribution for different values of Prandtl number $(Pr = 0.71, 1, 2, 7, 9, 11)$, radiation parameter $(N = 0.1, 0.5, 1, 3, 5, 7)$ and heat source parameter

$(Q = -2, -1, 0, 1, 2, 3)$ for dilatants, Newtonian fluids and pseudo plastics. Here it is observed that, velocity profile doesn't change with the change of parameters Pr, Q and *N* but increases as the power-law fluid index (n) increases.

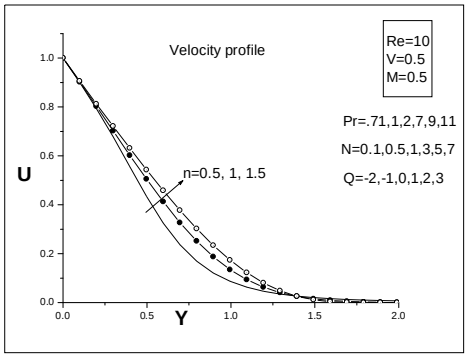

Fig. 3: Velocity profile for different values of Prandtl number (Pr) heat source parameter (Q) and radiation parameter (N) and power law fluid index (n)

Velocity profiles decreases as magnetic parameter (M) increases for all values of power-law fluid index (n) (Fig. 4). It is seen that the presence of magnetic field causes higher restriction to the fluid, which has reduced the fluid velocity. There is a steep fall in velocity in pseudo plastics $(n < 1)$ compare to other two types.

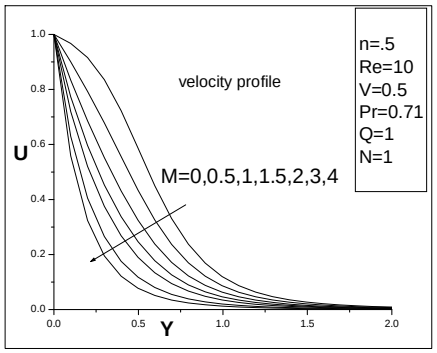

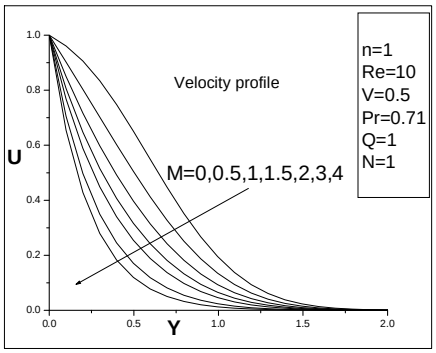

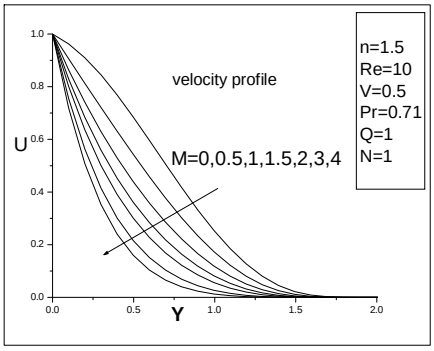

Fig.4: Effect of magnetic parameter (M) on velocity profile for different values on power law fluid index (n)

Temperature profile decreases as radiation parameter (N) increases (Fig. 5).We observe that, temperature profile reduces rapidly almost at an average rate of 5% with every increase of N from 0.1 up to 1. But as we increase N further, decreasing rate slows down. Due to radiation temperature rises quickly near the wall but then decreases immediately. Thus, temperature boundary layer can be controlled effectively using radiation parameter (N). Furthermore, heat transfer along the stretching sheet is faster when radiation is small.

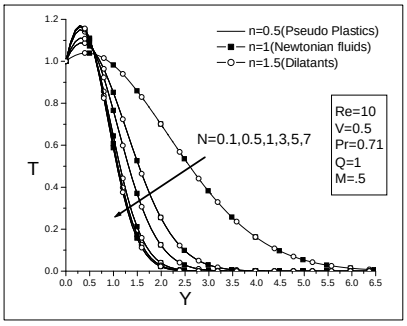

Fig. 5: Temperature profile for different values of radiation parameter (N) and power law fluid index (n)

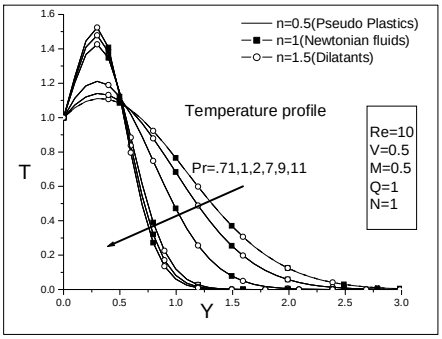

Fig. 6: Temperature profile for different values of Prandtl number (Pr) and power law fluid index (n)

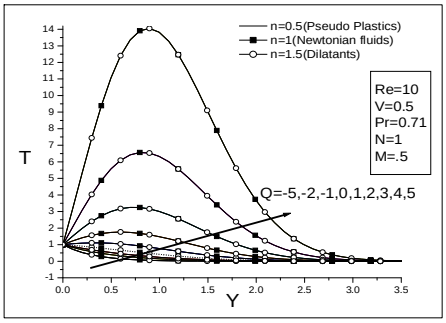

Fig. 7: Temperature profile for different values of heat source parameter (Q) and power law fluid index (n)

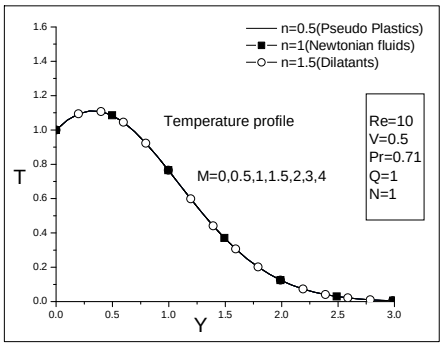

Fig. 8: Temperature profile for different values of magnetic parameter (M) and power law fluid index (n)

In forced convection, temperature profiles decrease with the increase of Prandtl number (Pr) (Fig.6). If we increase Pr from 0.71, the stretching sheet gain temperature from the environment but the heat gaining rate decreases. Every time we increase Pr, the temperature profile drops at an average rate 1.5%. When $Pr \geq 7$, heat gaining rate is almost zero that is thermal boundary layer doesn't change appreciably. However, temperature rises at the beginning of the flow for $Pr \geq 7$. Temperature profiles increase very rapidly, overshoot and stabilize as heat source parameter (Q) increases (Fig. 7). The dotted line represents the case without any heat generation or absorption. For $Q \geq 3$, temperature rises 2.5 times higher with every increase of Q . Due to heat generation initial wall temperature is very high. So that, the heat transfer rate is very low. In forced convection, temperature field remains unaffected by the change of magnetic parameter (M) (Fig.8) and power-law fluid index (n) (Fig.5-8).

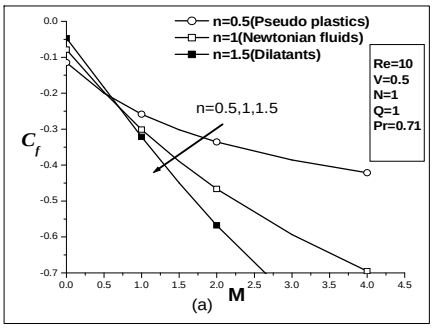

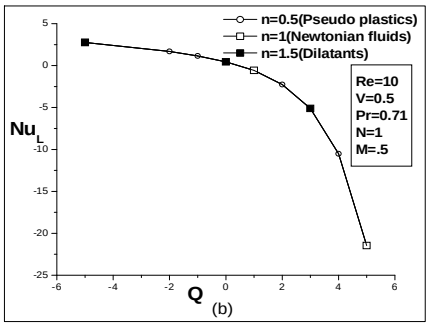

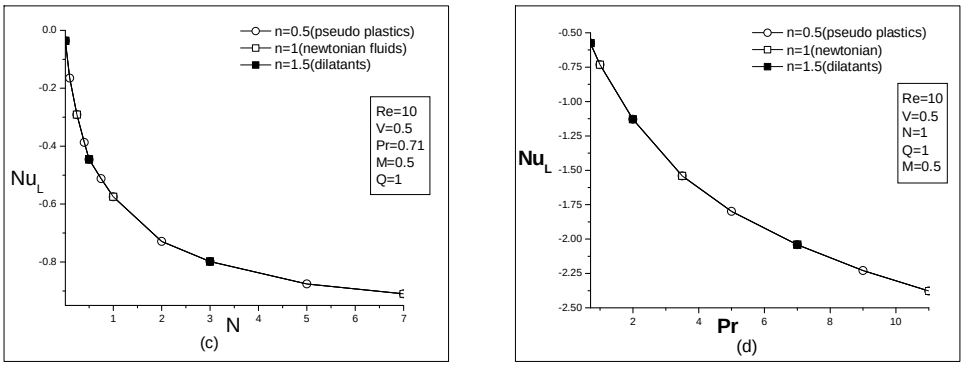

Fig. 9: Effect of (a) magnetic parameter (M) on skin friction coefficient (C_f) and (b) effect of heat source parameter (Q), (c) radiation parameter (N) (a) Prandtl number (Pr) on local Nusselt number (Nu_L) for different values of power-law fluid index (n).

Skin friction coefficient (C_f) decreases as both M and n increase (Fig.9 (a)). There is a cross flow near $M = 0.5$. Pseudo plastics have the least friction when magnetic parameter is high. Since in forced convection, the parameters Pr , Q and N showed no variation on velocity field (Fig.3), we get a constant skin friction which is $C_f = -0.19993$ for all values of Pr , Q and N .

The local Nusselt number (Nu_L) decreases as Q (Fig. 9(b)), N (Fig. 9(c)) and Pr (Fig.9 (d)) increase and remains constant to the change of n . Since there was no variation in temperature field (Fig.8) due to M , Nu_L remains unchanged for the variation of M . The value of Nu_L is -0.57486 . Negative value of Nu_L represents the heat absorption at the wall.

5. Conclusion

From the present study, the concluding remarks have been taken as follows:

- Prandtl number (Pr), heat source parameter (Q) and radiation parameter (N) have negligible effect on velocity profile because in forced convection, velocity field is independent of temperature field but it increases with the increase of power law fluid index (n). Velocity profile decreases as the magnetic parameter (M) increases for all values of n .
- Temperature profile increases as Q increases, decreases with the increase of both Pr and N and remains constant to the change of M and n .
- Skin friction coefficient (C_f) decreases as both M and n increase. (C_f) is same for all values of parameters pr, Q and N .
- The local Nusselt number (Nu_L) desreases as the parameters Pr, Q Q and N increase. (Nu_L) is same for all values of M and n .

REFERENCES

[1] Schowalter, W.R., "The application of boundary layer theory to power-law pseudo plastic fluid Similar solutions", AICHE J., (1960), 24-28.

[2] Banks W. H. H., "Similarity Solutions of the Boundary Layer Equations for a Stretching Wall", J. Mec. Theor. Appl., (1983), 375-392.

[3] Chen C. K., Char M. I., "Heat Transfer of a Continuous Stretching Surface with Suction or Blowing", J. Math. Anal. Appl., (1988), 568-580.

[4] Kishan Naikoti, Shashidar Reddy Borra, "Quasi-linearization Approach to MHD Effects on Boundary Layer Flow of Power-Law Fluids Past A Semi Infinite Flat Plate with Thermal Dispersion", Int. J. of Non-Linear Science, Vol.11, (2011), 301-311.

[5] Sahoo B., Poncet S., "Flow an heat transfer of a third grade fluid past an exponentially stretching sheet with partial slip boundary condition", Int. J. Heat Mass Transfer, (2011), 5010-50.

[6] Sajid M. and Hayat T., "Influence of thermal radiation on the boundary layer flow due to an exponentially stretching sheet", Int. J. Heat Mass Transfer, Vol. 35, (2008), 347-356.

[7] Elbashbeshy E.M.A. and Bazid M.A.A., Heat transfer over an unsteady stretching surface, J. Heat Mass Transfer., (2004), 1-4.

[8] Singh P., Jangid A., Tomer N.S., Sinha D., "Effects of thermal radiation and magnetic field on unsteady stretching permeable sheet in presence of free stream velocity", Int. J. Info. and Math. Sci., (2010).

[9] Gamal M., Abdel-Rahman , "Effects of variable viscosity and thermal conductivity on unsteady MHD flow of non-Newtonian fluid over a stretching porous sheet", Thermal science, Vol. 17, (2013), 1035-1047.

[10] Rohsenow, W.M., Harnett, "Handbook of Heat Transfer", 3rd edn. McGraw-Hill, J.P., Cho, Y.I., New York (1998).

NOMENCLATURE

Symbol		Description	Symbol		Description
K	-	The consistency coefficient,	q_r	-	The radioactive heat flux
U_0	-	Free stream velocity	C_f	-	Skin friction coefficient
g	-	The gravitational acceleration	Nu_L	-	The local Nusselt number
v_0	-	The velocity components in the y direction	C_p	-	The specific heat at constant pressure.
h	-	The convention heat transfer coefficient	u, v	-	The velocity components in the X and Y respectively
Q_0	-	The volumetric rate of heat generation/ absorption	x, y	-	Distance along X-axis and Y-axis respectively
B_0	-	The magnetic field	T	-	The temperature of the field
n	-	Power-law fluid index	Y	-	Dimensionless length
k_e	-	The mean absorption coefficient	T	-	Dimensionless temperature
Q	-	The heat source parameter	t	-	Dimensionless time
M	-	The magnetic parameter	L	-	The characteristic length
N	-	The radiation parameter	t	-	Time
Re	-	The local Reymolds number	Δx *or* h	-	Mesh size along X-axis
Pr	-	The generalized Prandtl number	Δt *or* k	-	Mesh size along Y-axis
N_x, N_t	-	Maximum number of grid spacing in X-axis and Y-axis respectively	U, V	-	Dimensionless velocity components along X-axis and Y-axis respectively

Greek symbols

ρ	-	The density of the fluid	α	-	The thermal diffusivity
σ	-	The electric conductivity	τ	-	The shear stress
κ	-	The thermal conductivity of the fluid	σ	-	Boltzmann constant-Stephen

Subscripts

w	-	At the wall	∞	-	In the free stream
x, y	-	Component along X-axis and Y-axis respectively	j	-	Grid point with x co-ordinates and y co-ordinates